energies

MDPI

Article

Effect of the Cathodic Gas Diffusion Layer on the Performance of a Proton Exchange Membrane Electrolyzer

Daniela Lorena Canelas Montaño †, Pablo Ruiz García †, Andrés Jerez Navarro †, Modesto Aguirre Gomez † and José Javier López Cascales *,†

Departamento Ingeniería Quimíca y Ambiental, Universidad Politécnica de Cartagena, Campus Alfonso XIII, Aulario C, 30203 Cartagena, Murcia, Spain; daniela-canelas@hotmail.com (D.L.C.M.); pabloruizgarcia8@gmail.com (P.R.G.); andres1994f@gmail.com (A.J.N.); modestoaguirre@hotmail.com (M.A.G.)

* Correspondence: javier.lopez@upct.es

† These authors contributed equally to this work.

Abstract: Hydrogen production through electrolysis using renewable resources is highly promising for reducing greenhouse gas emissions. While significant efforts have focused on developing more efficient and cost-effective catalysts to lower hydrogen production costs, catalysts are not the primary expense in electrolyzer fabrication. In the case of Proton Exchange Membrane Water Electrolyzers (PEMWEs), other components—such as the proton membrane, gas diffusion layer (GDL), and bipolar plates—contribute more to overall costs. To explore this, a study was conducted on the performance of PEMWEs with various carbon paper GDLs, developed in the lab, on the cathodic side. This study examined how properties like electrical conductivity, porosity, and gas permeability affect performance. These findings emphasize the need to optimize components beyond catalysts to improve the cost-effectiveness of hydrogen production through electrolysis.

Keywords: PEMEC; GDL; morphology; performance

check for updates

Citation: Canelas Montaño, D.L.; Ruiz García, P.; Jerez Navarro, A.; Aguirre Gomez, M.; López Cascales, J.J. Effect of the Cathodic Gas Diffusion Layer on the Performance of a Proton Exchange Membrane Electrolyzer. *Energies* **2024**, *17*, 5298. https://doi.org/10.3390/en17215298

Academic Editor: Antoni Zywczak

Received: 28 August 2024
Revised: 18 October 2024
Accepted: 21 October 2024
Published: 25 October 2024

Copyright: © 2024 by the authors. Licensee MDPI, Basel, Switzerland. This article is an open access article distributed under the terms and conditions of the Creative Commons Attribution (CC BY) license (https://creativecommons.org/licenses/by/4.0/).

1. Introduction

The increasing emissions of greenhouse gases and the economic challenges stemming from global fossil fuel shortages have positioned electrolytically produced hydrogen as a promising and efficient solution to both issues [1]. Among the available technologies, Proton Exchange Membrane Water Electrolysis (PEMWE) is particularly attractive for sustainable hydrogen production [2]. However, one of the major barriers hindering the widespread adoption of this technology is the high production cost of hydrogen, especially when compared to the more conventional method of hydrogen production via natural gas reforming.

Much of the current research has been dedicated to the development of more cost-effective catalysts for electrolyzers, largely because these systems often use rare and noble metals like iridium, ruthenium, and platinum, which are both scarce and expensive. Improving the redox morphology of these precious metals to enhance their electrocatalytic properties has been a major area of focus in research [3–6].

However, while catalyst development is crucial, it is important to note that the overall impact of catalyst cost on the total capital cost of an electrolyzer is relatively modest. Other components, such as titanium bipolar plates, interconnectors, proton exchange membranes, and gas diffusion layers (GDLs or PTLs), significantly contribute to the overall cost. Therefore, a comprehensive cost-reduction strategy, addressing all components, is necessary to enable the widespread adoption of hydrogen production via electrolysis [7].

Focusing on the gas diffusion layer (GDL), these components play a critical role in the electrolyzer's core by requiring high electrical conductivity, high porosity, and chemical stability under electrolyzer operating conditions. Recently, there has been considerable interest in enhancing these properties to optimize GDL performance in electrolyzers [8–10].

Various experimental and theoretical studies have investigated the effects of pore distribution on GDL performance. For instance, Zhang et al. [11] demonstrated that hydrophobicity and pore gradient distribution affect proton electrolyte membrane fuel cells (PEMFCs) and proton electrolyte membrane water electrolyzers (PEMWEs) differently. While hydrophobic GDLs improve PEMFC performance, hydrophilic GDLs enhance PEMWE performance. Another critical property is pore tortuosity, which limits optimal GDL performance by restricting the movement of bubbles and water inside the GDL [12].

Traditionally, carbon paper GDLs have been excluded from the anode side of electrolyzers due to chemical instability caused by oxidation of the carbon material [11]. This has led to the prevalent use of titanium GDLs, especially for the anode side [11]. Despite the different operational requirements of the anode and cathode, many electrolyzers are symmetrically assembled using titanium GDLs on both sides [2,7].

In this study, we examine the performance of various carbon paper GDLs on the cathode side of a single-cell proton exchange membrane electrolyzer (PEMWE). These GDLs were fabricated in our laboratory following established procedures [13], using different natural fibers that impart varying properties such as electrical conductivity, gas permeability, and pore distribution. An ex-situ characterization of these cathodic GDLs was conducted. The results show that by varying the type of natural fiber used in GDL fabrication, we can manipulate the pore distribution profile of the GDLs. This adjustment of pore distribution and tortuosity plays a crucial role in electrolyzer performance, outweighing the influence of electrical conductivity. Additionally, the adoption of these innovative carbon-paper GDLs led to a significant cost reduction of 45% in the electrolyzer assembly, particularly when compared to the use of titanium GDLs on both the cathode and anode sides.

2. Experimental

2.1. GDL Preparation

The GDLs used in this work were prepared following the same procedure that was described elsewhere [13]. With the objective of producing GDLs with different porous morphology, two different natural fibers were used to prepare the GDLs: cotton fibers and esparto grass fibers. Thus, due to the different structures of both fibers, such as can seen in Figure 1, GDLs with different porous morphology were generated during their fabrication process.

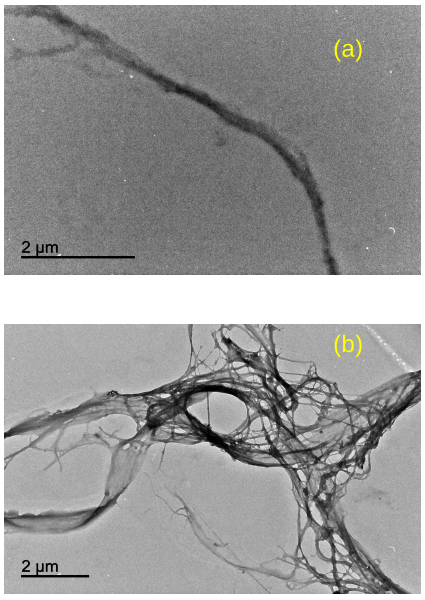


Figure 1. TEM images of The two different fibers used in this work are cotton fibers (**b**) and esparto grass fibers (**a**). The esparto grass fibers exhibit a linear, wire-like structure, in contrast to the branched, more intricate structure of the cotton fibers

In this sense, two different GDLs were prepared, corresponding to the cotton GDL (GDL-c) and esparto GDL (GDL-e). Those GDLs were compared with a titanium-felt GDL-Ti, provided by Hydrogreen Energy S.L. (www.hydrogreenenergy.com, accessed on 1 July 2023).

Figure 2 shows the SEM images of the three GDLs studied in this work. Thus, Figure 2 shows the different morphology existing between GDL-Ti and the two GDLs fabricated using natural fibers. From the images of Figure 2, we see the evident different morphology existing between the GDL-Ti and the other two GDLs.

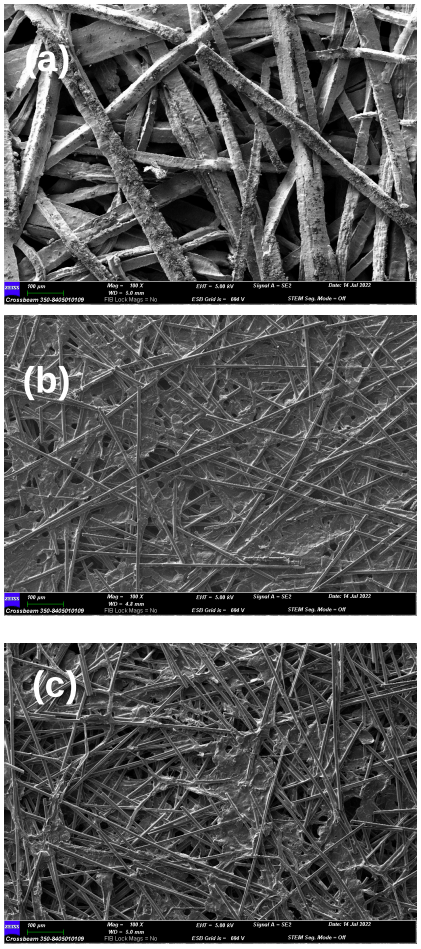


Figure 2. SEM images of the four types of GDL used in this study: (**a**) GDL-Ti, (**b**) GDL-c, and (**c**) GDL-e. For further information, see the text.

2.2. Electrodes Preparation

For electrode preparation, two different inks were generated. The anodic catalyst ink was prepared with 0.32 g of Black iridium, 5 mL 2-propanol, 0.016 mL epoxy containing 700 ppms of graphene, and 1.5 mL of Nafion solution 5% (Alfa Aesar, Haverhill, MA, USA). The cathodic catalyst ink was prepared with 0.32 g Pt/C 20%, 7 mL 2-isopropanol, 1.5 mL of Nafion solution 5% (Alfa Aesar), and 0.016 mL epoxy with 700 ppm of graphene. Since both catalytic inks were prepared, they were subjected to ultrasound for 1 h and then stirred for 24 h before use.

Once the catalytic inks were ready for use, the catalyst was deposited onto a silicon paper, generating a thing catalyst layer. Next, the catalyst layer was transferred to the membrane by a hot-press procedure at 130 degrees Celsius and 106 kg/cm^2 for 3 min. Thus, a final catalyst concentration of 2.5 mg/cm^2 of Black iridium on the anode side and 0.8 mg/cm^2 platinum on the cathode side was obtained.

Finally, the MEAs were generated by hot-press of the three different GDLs on the catalyst layers under analog hot-press conditions than the described above.

2.3. Electrolyzer

A single-cell electrolyzer was studied. In this regard, Figure 3 shows the elements that compose the single cell. In this regard, both plates and the big mesh were of titanium. An additional stainless mesh was added to the cathode side to improve the electric contact with the GDL. Finally, an image of the MEA prepared following the above procedure was included in Figure 3.

In this regard, the electrolyzer was coupled to an external heater to maintain a constant temperature of 80 degrees Celsius in the cell.

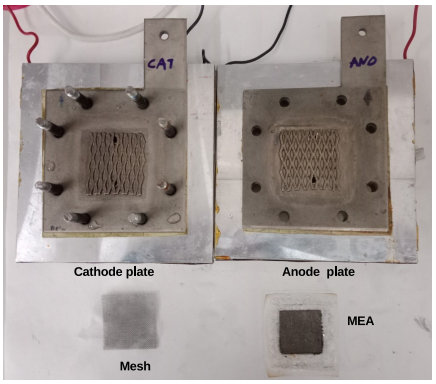


Figure 3. Single-cell electrolyzer components and MEA. Cathode and anode plate were fabricated in titanium. A stainless mesh was additionally used on the cathode side of the electrolyzer.

3. Results and Discussion

3.1. GDL Porosity

GDLs play a crucial role regulating the flux of water and gases from and to the catalyst face in a PEMWE. In this regard, the pore diameter and pore distribution function are going to affect the flux of water and gases by the dimensions of the pore diameters. Thus, the response of the electrolyzer is going to be modulated by the pore distribution in the electrolyzer. In this context, Figure 4 shows the pore distribution functions of the three different GDLs studied in this work.

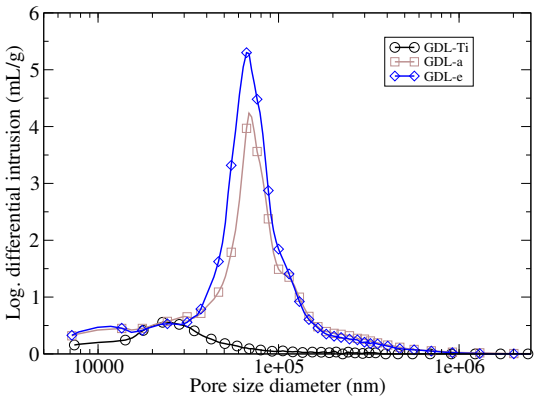


Figure 4. Pore distribution function of the GDLs measured with mercury porosimetry.

Figure 4 shows the clear difference in pore distribution between the commercial titanium felt and the other three GDLs produced with different natural fibers. In this regard, the maximum of the pore distribution functions of the titanium felt GDL is around 25 µm, which contrasts with the value of 68 µm for the other two GDLs. In this regard, Table 1 shows the porosity and mean pore diameter of the GDLs studied in this work.

Table 1. Porosity and pore diameter determined by mercury porosimetry.

GDL	GDL-Ti	GDL-c	GDL-e
Porosity (%)	59	76	81
Pore diameter (4V/A) (μm)	2.5	14.8	18.2

Table 1 shows that GDLs fabricated with natural fibers provide high porosity to the GDL. Furthermore, the presence of esparto fibers in the GDL composition enhances the porosity in the GDL, which is associated with the nature of its fiber topology in comparison with the cotton fibers that are more branched. This difference in the fiber topology is translated to a variation in the GDL porosity, passing from a mean pore diameter of 14.8 μm in the GDL-c to 18.2 μm for the GDL-e, which represents an increase of 23% in the pore diameter. In line with this result, the presence of esparto grass fibers also increased the porosity of the GDL in a 6.5%. Thus, by the proper selection of the natural fiber used for the GDL preparation, we are able to generate different GDLs with different pore morphologies.

3.2. GDL Permeability

The permeability of the GDLs to gases is a property that is narrowly related to its pore morphology [13]. In this regard, although this property is in part related to the net porosity of a gas diffusion layer, this is only partially true because the gas permeability is mainly associated with the pore morphology, while porosity is related to the void volume inside the GDL. In our case, the permeability was measured using the Gürley method, such as described in the UNE Norm 57066-3:2003. [14] Thus, the permeability of the three GDLs studied were 12.5, 21.9, and 31.5 cm/s for the GDL-c, GDL-e, and GDL-Ti, respectively. In this regard, we observe how the type of natural fiber employed in the GDL preparation greatly modifies the permeability of the two GDLs generated with natural fibers.

3.3. Electrical Conductivity

A gas diffusion layer presents an anisotropic structure due to the different orientations of the fibers in and through the plane. Hence, two electrical conductivities must be specified to characterize its electrical conductivity. The electrical conductivity in the plane was measured using the linear four points method, with a distance of 5 mm between two consecutive points. This method consists of determining the potential difference between two points due to the application of an electrical current between the other two, maintaining constant the distance between consecutive points [15,16]. Thus, the electrical resistivity in the plane can be measured as follows [15]:

$$\rho_{in} = \frac{\pi t}{\ln 2} \frac{V}{I} \quad (1)$$

where t is the sample thickness, I the electrical current applied between the two external points, and V the electrical potential measured between the other two points. Hence, the electrical conductivity, σ_{in}, can be obtained as follows:

$$\sigma_{in} = \frac{1}{\rho} \quad (2)$$

where σ_{in} is expressed in S/m.

The through-plane electrical resistivity, ρ_T, was obtained from Equation (3) ([17]):

$$R_T = \frac{\rho_T \cdot l}{A} \quad (3)$$

where R_T is the electrical resistance of a sample confined between two copper plates with a golden bath, under a pressure of 10 kg/cm^2 and measured with a miniOhmeter BK-Precision BA6010 at 1 kHz, ρ_T is the resistivity expressed as Ohms.cm, A is the transversal

surface, and l the sample thickness. Thus, the through-plane conductivity, σ_T, corresponds to the inverse of ρ_T, $\sigma_T = \frac{1}{\rho_T}$, and its units are S/cm.

Table 2 shows the electrical conductivities of the three GDLs studied. In general, we see, as in line with the expected, that an increase in porosity introduces a diminishing in the electrical conductivity. Thus, as a consequence of the increase in porosity of the GDL-e with respect to the GDL-c, a diminution in the electrical conductivity was measured both in and through the plane. Obviously, due to the metallic nature of the GDL-Ti, its electrical conductivity is much higher than that obtained in both GDLs with natural fibers.

Table 2. In and through the plane electrical conductivity.

Conductivity	GDL-Ti	GDL-c	GDL-e
σ_{in} (S/m)	188,721 ± 3500	6740 ± 690	6973.2 ± 400
σ_T (45 kg/cm^2)	1.628 ± 0.006	4.11 ± 0.05	1.51 ± 0.02
σ_T (76 kg/cm^2)	1.425 ± 0.004	4.75 ± 0.15	2.16 ± 0.04
σ_T (106 kg/cm^2)	1.231 ± 0.003	5.11 ± 0.14	2.72 ± 0.08

3.4. Hydrophobicity

GLD plays an important role in the electrolyzer evacuating the oxygen and hydrogen generated during the redox process on the catalyst surface, connecting the catalyst to the external source, and distributing the water on the anode catalyst surface. Hence, it seems obvious that hydrophobicity, together with the porosity of the GDL (properties that are related each other [18]), are key properties for water managing in a PEME [19].

Figure 5 shows the contact angle of a water droplet with the surface of the three GDLs. From the contact angle, we see how both GDLs fabricated with natural fibers show a contact angle of around 140 degrees in comparison to the 60 degrees of the GDL-Ti. That result evidences a clear difference in hydrophobicity between both GDLs with natural fiber, in comparison with the hydrophilic behavior of the GDL-Ti. Hence, in this sense, it seems that the hydrophobicity of the GDLs, together with their porosity (properties that are related to each other in a certain way [18]) are two critical properties for managing the water and gases generated inside the electrolyzer [19].

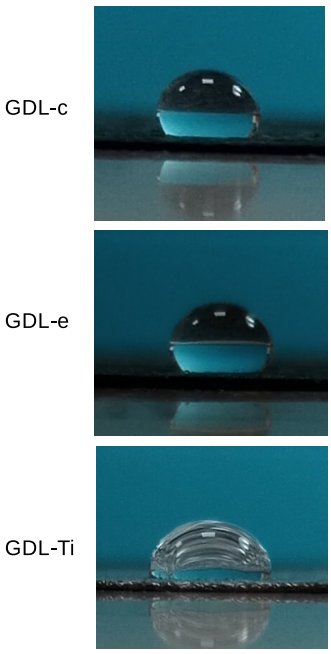


Figure 5. Contact angle of a water droplet on the surface of the three GDLs studied in this work: GDL-c with cotton fibers, GDL-e with esparto fibers, and GDL-Ti titanium-felt.

3.5. Polarization Curves

Figure 6 provides information of the polarization curves of the three electrolyzers with different GDLs on the cathode side. Thus, from such figures, we observe how the GDL-e provides the best performance of the three GDLs studied.

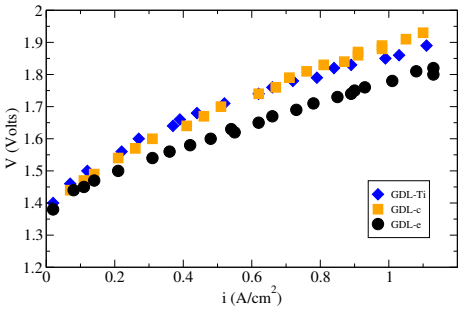


Figure 6. Polarization curves corresponding to the three different electrolyzers assembled with the three different cathodic GDLs studied in this work.

Thus, from Figure 6, we see how the electrolyzer containing a GDL-Ti shows similar performance to the electrolyzer with a GDL-c, in spite of the excellent electrical conductivity and permeability of the GDL-Ti. This difference is even more notable when the performance of the electrolyzer with a GDL-Ti is compared with the corresponding GDL-e.

4. Conclusions

The new gas diffusion layers made from natural fibers showed a competitive advantage over the use of high-cost titanium mesh layers, without losing electrolyzer performance. In this sense, we demonstrated that an optimal pore distribution in the cathodic gas diffusion layer plays an important role in the final electrolyzer response, this property being even more critical than electrical conductivity in a GDL for optimal PEMWE performance.

The results depicted in this work emphasize the benefits of using natural fibers for gas diffusion layers (GDLs) in proton exchange membrane water electrolyzers (PEMWEs), such as we enumerate below:

1. Sustainability and Cost Reduction: Using natural fibers in GDLs is presented as a more sustainable and cost-effective solution compared to traditional materials, particularly expensive titanium mesh layers. This addresses one of the major challenges in electrolyzer fabrication: high production costs.
2. Performance Maintenance: The results indicate that these natural fiber-based GDLs maintain comparable performance to traditional titanium layers. This is an important finding because it suggests that the cost reduction does not come at the expense of efficiency or effectiveness.
3. Pore Distribution vs. Electrical Conductivity: This study suggests that the pore distribution within the GDL plays a more crucial role than its electrical conductivity for achieving optimal PEMWE performance. This highlights the importance of designing GDLs with the right pore structure to ensure efficient gas diffusion and overall electrolyzer operation.

Overall, this work advocates for natural fiber GDLs as both a competitive and environmentally friendly alternative in PEMWE technology, with optimized pore distribution being key to their success.

Author Contributions: A.J.N. and M.A.G. prepared the samples. D.L.C.M. and P.R.G. prepared and analyzed the performance of the samples in the electrolyzer. J.J.L.C. coordinated and scheduled the work and wrote the manuscript. All authors have read and agreed to publish the actual version of this manuscript.

Funding: J.J.L.C. acknowledges the grant CPP2022-010018 financed through the project MCIN/AEI/10.13039/501100011033 and the European Union "NextGenerationEU"/PRTR".

Data Availability Statement: The original contributions presented in the study are included in the article, further inquiries can be directed to the corresponding author.

Conflicts of Interest: The authors declare no conflicts of interest.

References

1. Busby, R.L. *Hydrogen and Fuel Cells*; Pennwell Publishing: Tulsa, OK, USA, 2005.
2. Kumar, S.; Himabindu, V. Hydrogen production by pem water electrolysis: A review. *Mater. Sci. Energy Technol.* **2019**, *2*, 442–454. [CrossRef]
3. Blasi, A.; D'Urso, C.; Vaglio, V.; Antonucci, V.; Arico, A.; Ornelas, R.; Matteucci, F.; Orozco, G.; Beltran, D.; Meas, Y.; et al. Preparation and evaluation of ruo2–iro2, iro2–pt and iro2–ta2o5 catalysts for the oxygen evolution reaction in an spe electrolyzer. *J. Appl. Electrochem.* **2009**, *39*, 191–196. [CrossRef]
4. Reiera, T.; Weidingerb, I.; Hildebrandtb, P.; Kraehnerta, R.; Strassera, P. Electrocatalytic oxygen evolution reaction on iridium oxide model film catalysts: Influence of oxide type and catalyst substrate interactions. *ECS Trans.* **2013**, *58*, 39–51. [CrossRef]
5. Reier, T.; Teschner, D.; Lunkenbein, T.; Bergmann, A.; Selve, S.; Kraehnert, R.; Schlögl, R.; Strassera, P. Electrocatalytic oxygen evolution on iridium oxide: Uncovering catalyst-substrate interactions and active iridium oxide species. *J. Electrochem. Soc.* **2014**, *161*, F876–F882. [CrossRef]
6. Jiang, H.; Ge, S.; Zhang, Y.; Dong, M.; Wu, S.; Wu, M.; Zhang, J.; Ge, R.; Guo, Z. Self-supported iridium oxide nanostructures for electrocatalytic water oxidation in acidic media. *J. Phys. Chem. C* **2020**, *124*, 2–8. [CrossRef]
7. Zhang, L.; Zhao, H.; Wilkinson, D.; Sun, X.; Zhang, J. (Eds.) *Electrochemical Water Electrolysis*. Fundamentals and technologies; CRC Press: Boca Raton, FL, USA, 2020.
8. Omrani, R.; Shabani, B. Gas diffusion layer modifications and treatments for improving the performance of proton exchange membrane fuel cells and electrolysers: A review. *Int. J. Hydrogen Energy* **2017**, *42*, 28515–28536. [CrossRef]
9. Hussain, J.; Kim, D.; Park, S.; Khalid, M.; Hussain, S.; Lee, B.; Song, M.; Kim, T. Porous material (titanium gas diffusion layer in proton exchange membrane fuel cell/electrolyzer: Fabrication method and geodict: A critical review. *Materials* **2023**, *16*, 4515. [CrossRef]
10. Yan, S.; Yang, M.; Sun, C.; Xu, S. Liquid water characteristics in the compressed gradient porosity gas diffusion layer of proton exchange membrane fuel cells using the lattice boltzman method. *Energies* **2023**, *16*, 6010. [CrossRef]
11. Zhang, T.; Meng, L.; Chen, C.; Du, L.; Wang, N.; Xing, L.; Tang, C.; Hu, J.; Ye, S. Similarities and differences between gas diffusion layers used in proton exchange membranes fuel cell and water electrolysis for material and mass transport. *Adv. Sci.* **2024**, *11*, 2309440. [CrossRef] [PubMed]
12. Arbabi, F.; Lalantarian, A. Feasibility study of using microfluidic platforms from visualizing bubble flows in electrolyzers gas diffusion layers. *J. Power Sources* **2014**, *258*, 142–149. [CrossRef]
13. Navarro, A.J.; Gómez, M.A.; Daza, L.; López-Cascales, J.J. Production of gas diffusion layers with cotton fibers for their use in fuel cells. *Sci. Rep.* **2022**, *12*, 4219–4229. [CrossRef] [PubMed]
14. Determination of Air Permeance. Part 3: Gurley Method. Available online: https://www.une.org/encuentra-tu-norma/busca-tu-norma/norma?c=N0030415 (accessed on 27 August 2024).
15. Miccoli, I.; Edler, F.; Pfnür, H.; Tegenkamp, C. The 100th anniversary of the four-point probe technique: The role of probe geometries in isotropic and anisotropic systems. *J. Phys. Condens. Matter* **2015**, *27*, 223201–223230. [CrossRef] [PubMed]
16. Alarifi, I. Investigation the conductivity of carbon fiber composites focusing on measurement techniques under dynamic and static loads. *J. Mater. Res. Technol.* **2019**, *8*, 4863–4893. [CrossRef]
17. Cooper, K. Characterizing throgh-plane and in-plane ionic conductivity of polymer electrolyte membranes. *ECS Trans.* **2011**, *41*, 1371–1380. [CrossRef]
18. Cassie, A.; Baxter, S. Wettability of porous surfaces. *Faraday Soc.* **1944**, *40*, 546–551. [CrossRef]
19. Lapicque, F.; Belhadj, M.; Bonnet, C.; Pauchet, J.; Thomas, Y. A critical review on gas diffusion micro and macroporous layers degradations for improved membrane fuel cell durability. *J. Power Sources* **2016**, *336*, 40–53. [CrossRef]

Disclaimer/Publisher's Note: The statements, opinions and data contained in all publications are solely those of the individual author(s) and contributor(s) and not of MDPI and/or the editor(s). MDPI and/or the editor(s) disclaim responsibility for any injury to people or property resulting from any ideas, methods, instructions or products referred to in the content.